J|A|C|S
ARTICLES
Published on Web 01/23/2007

The Crystal Structures of the Calcium-Bound con-G and con-T[K7γ] Dimeric Peptides Demonstrate a Metal-Dependent Helix-Forming Motif

Sara E. Cnudde,[†] Mary Prorok,[‡] Qiuyun Dai,[‡] Francis J. Castellino,*[,‡] and James H. Geiger*[,§]

Contribution from the Department of Biochemistry, Michigan State University, East Lansing, Michigan 48824, Department of Chemistry and Biochemistry and W. M. Keck Center for Transgene Research, University of Notre Dame, Notre Dame, Indiana 46556, and Department of Chemistry, Michigan State University, East Lansing, Michigan 48824

Received August 14, 2006; E-mail: geiger@cem.msu.edu; fcastell@nd.edu

Abstract: Short peptides that have the ability to form stable α-helices in solution are rare, and a number of strategies have been used to produce them, including the use of metal chelation to stabilize folding of the backbone. However, no example exists of a structurally well-defined helix stabilized exclusively through metal ion chelation. Conantokins (con)-G and -T are short peptides that are potent antagonists of *N*-methyl-D-aspartate receptor channels. While con-G exhibits no helicity alone, it undergoes a structural transition to a helical conformation in the presence of a variety of multivalent cations, especially Mg^{2+} and Ca^{2+}. This complexation also results in antiparallel dimerization of two peptide helices in the presence of Ca^{2+}, but not Mg^{2+}. A con-T variant, con-T[K7γ], displays very similar behavior. We have solved the crystal structures of both Ca^{2+}/con-G and Ca^{2+}/con-T [K7γ] at atomic resolution. These structures clearly show the nature of the metal-dependent dimerization and helix formation and surprisingly also show that the con-G dimer interface is completely different from the con-T[K7γ] interface, even though the metal chelation is similar in the two peptides. This represents a new paradigm in helix stabilization completely independent of the hydrophobic effect, which we define as the "metallo-zipper."

Introduction

Knowledge of the interactions that stabilize local protein structure is critical for a global understanding of protein folding. To this end, much effort has been invested in resolving the physical and chemical principles that direct the formation of the α-helix, the most widespread secondary structural motif, and its supersecondary and tertiary structural derivates, which include coiled coils and helix bundles. Short (∼20 residues) linear peptides corresponding to structured segments of naturally occurring proteins would clearly be instructive in this regard, owing to the ease with which their primary sequences can be manipulated and their structures interpreted. However, except for a few notable examples,[1,2] such abbreviated protein segments, when examined in isolation in aqueous milieu, rarely adopt the conformations observed within the context of the full-length protein. The de novo peptide/protein design field has largely emerged to overcome this problem, and considerable success has been achieved in the design of peptides that are sufficiently short to be synthetically practical, yet capable of adopting stable helices that can further organize into higher order complexes. However, most of these motifs do not have biological relevance. Among the various strategies that have been employed for directing the formation of monomeric and/or interacting helices, the most tractable and effective approach involves the use of metal ions. For instance, helix nucleation and the attendant folding of unstructured or partially structured peptides can be readily facilitated through metal ion bridging of appropriately spaced natural and unnatural metal-binding amino acids.[3−6] In these particular cases, introduction of the metal induces 80−90% helicity in a 17-mer[3,4] and more than 80% helicity in an 11-residue peptide,[5] depending on the metal ion. Similarly, bridging interactions have been exploited to stabilize contacts between two or more helical strands. Many of these studies have focused on the metal-assisted assembly of prefolded de novo structures via pendent metal ligands, namely porphyrin and bipyridyl derivatives.[7,8]

A more daunting challenge in the de novo construction of higher order structures involves the metal-assisted organization of random coils into helix−helix assemblies. This has been

[†] Department of Biochemistry, Michigan State University.
[‡] University of Notre Dame.
[§] Department of Chemistry, Michigan State University.

(1) Brown, J. E.; Klee, W. A. *Biochemistry* **1971**, *10*, 470−476.
(2) Siedlecka, M.; Goch, G.; Ejchart, A.; Sticht, H.; Bierzyski, A. *Proc. Natl. Acad. Sci. U.S.A.* **1999**, *96*, 903−908.
(3) Ghadiri, M. R.; Choi, C. *J. Am. Chem. Soc.* **1990**, *112*, 1630−1632.
(4) Ghadiri, M. R.; Fernholz, A. K. *J. Am. Chem. Soc.* **1990**, *112*, 9633−9635.
(5) Ruan, F.; Chen, Y.; Hopkins, P. B. *J. Am. Chem. Soc.* **1990**, *112*, 9403−9404.
(6) Wade, H.; Stayrook, S. E.; Degrado, W. F. *Angew. Chem.* **2006**, *45*, 4951−4954.
(7) Ghosh, D.; Pecoraro, V. L. *Inorg. Chem.* **2004**, *43*, 7902−7915.
(8) Doerr, A. J.; McLendon, G. L. *Inorg. Chem.* **2004**, *43*, 7916−7925.

10.1021/ja065722q CCC: $37.00

accomplished by induction of a triple-stranded coiled coil following transition metal ion binding to His or Cys residues contained within a four heptad repeat peptide of a random structure.[9,10] Furthermore, design of Zn^{2+}-chelating sites into a model four-helix bundle resulted in a highly stabilized, ordered structure compared to the apo-variant.[11] A particularly dramatic example of metal ion-induced folding was the design of two disulfide-linked 35-mers that underwent a random coil to coiled coil transition in the presence of various metal ions.[12] The molecular interactions pivoting this self-organization involve interstrand metal ion bridges between γ-carboxyglutamate (Gla) residues occupying positions *e* and *g* in the α-helical heptad repeat. In all of these examples, the metal ion is crucial to initiating strand association, but the predominant forces driving and stabilizing the complex formation rely on interstrand hydrophobic contacts. In some of these studies, covalent bonds between the helix-forming strands are necessary for complex stabilization.[11,12] Hence, the metal ion-triggered association of peptide chains in these instances cannot be regarded as fully autonomous. Additionally, structural characterization of such complexes has proven elusive, raising questions as to the precise nature of stabilizing interhelix interactions.

We have recently acquired evidence to suggest that the challenge of generating a small, unstructured peptide capable of metal ion-triggered helix formation and self-association has been satisfied by nature.[13] The peptide, conantokin-G (con-G), is a component of the venom of the predatory marine snail, *Conus geographus*.[14] In mammals, con-G antagonizes ion flow through the *N*-methyl-D-aspartate (NMDA) subtype of ionotropic glutamate receptors, the dysfunction of which is linked to numerous chronic and acute neuropathologies.[15] con-G is 17 amino acids in length and contains five Gla residues at positions 3, 4, 7, 10, and 14. Of these, only Gla4 is absolutely required for NMDA receptor activity.[16] While a variety of di- and trivalent metals can promote a conformational change from random coil to a helix, only Ca^{2+} allows for the formation of a dimeric con-G complex.[13] Thiol-disulfide rearrangement experiments with Cys-containing con-G variants are congruous with an antiparallel alignment of peptide chains in the Ca^{2+}-containing dimer, and Ala replacement studies have confirmed the participation of Gla residues 3, 7, 10, and 14 in the dimerization event. From these data, we proposed a model for the complex in which antiparallel con-G strands are stabilized solely through Ca^{2+} bridging of Gla headgroups within the helix−helix interface. This model represents a heretofore unknown motif among naturally occurring proteins or peptides.

A second member from the conantokin family, conantokin-T (con-T), shares some sequence identity to con-G at 8 of 21 residues including four Gla residues at positions 3, 4, 10, and 14. However, several primary and secondary structural differences exist between con-G and con-T, specifically at position 7, which is occupied by Lys in con-T and Gla in con-G. While con-T does not undergo Ca^{2+}-induced self-assembly, previous studies have shown that replacing the Lys at position 7 with a Gla (con-T[K7γ]) allows the peptide to form an antiparallel helix dimer in the presence of Ca^{2+}.[17]

The unique and novel interactions proposed for conantokin helix self-assembly have motivated an atomic resolution structural analysis to elucidate the interfaces between dimeric helices. An understanding of this novel interface will result in new approaches to rational and readily dissociable design of local intraprotein motifs and specifically constructed multimeric protein structures. To this end, we have determined X-ray structures of Ca^{2+}-complexed con-G and con-T[K7γ] at high resolution (1.2 Å for Con-G and 1.6 Å for con-T[K7γ]). This structural information will be valuable in rational drug design for these particular neuroactive peptides, and extension of this knowledge will allow the development of structural models for metal ion-stabilized α-helical regions of proteins and manipulation of protein folding. These results also provide structural models of Gla-rich domains of vitamin K-dependent proteins and the structural transitions that accompany the binding of divalent cations to these modules. The salient features of this investigation are summarized herein.

Materials and Methods

Peptide Synthesis, Purification, and Characterization. con-G and con-T[K7γ] were synthesized, purified, and characterized as previously described.[13] The amino acid sequences of the peptides relevant to this article, as well as their α-helical heptad repeat assignments, are shown below:

	b c d e f g a b c d e f g a b c d e f g a
con-G	**G-E-γ-γ-L-Q-γ-N-Q-γ-L-I-R-γ-K-S-N-NH_2**
con-T	**G-E-γ-γ-Y-Q-K-M-L-γ-N-L-R-γ-A-E-V-K-K-N-A-NH_2**
con-T[K7γ]	**G-E-γ-γ-Y-Q-γ-M-L-γ-N-L-R-γ-A-E-V-K-K-N-A-NH_2**

Crystallization. The lyophilized con-G and con-T[K7γ] were dissolved in 50 mM $CaCl_2$ and 100 mM Tris-HCl, pH 8, to a concentration of 10 mg/mL. Crystals of con-G were grown at room temperature by the hanging drop vapor diffusion method in 35% dioxane, and crystals appeared within 24 h. Crystals of con-T[K7γ] were similarly grown at 4 °C in 3 M $(NH_4)_2SO_4$ and 0.1 M NaOAc, pH 5.5, and crystals appeared after 1 year.

Data Collection. Crystals of con-G were briefly soaked in a solution containing 35% dioxane and 30% MPD at room temperature and flash frozen by immersion in liquid N_2. Data were collected at the Advanced Photon Source COM-CAT 32-ID at Argonne National Laboratory to a resolution of 1.2 Å and were processed and scaled using the HKL suite of programs[18,19] in the tetragonal space group $P4_222$. The crystal to detector distance was 60 mm, and 200° of data were collected with an oscillation of 1°. The crystal parameters and data collection statistics of con-G are listed in Table 1.

Crystals of con-T[K7γ] were briefly soaked in a solution containing 4 M NaH_2PO_4/20% glycerol, pH 5.5, at 4 °C and flash frozen by immersion in liquid N_2. Data were also collected at COM-CAT32ID to a resolution of 1.6 Å and processed and scaled using AUTOMAR in the cubic space group $P4_332$. The crystal to detector distance was 100 mm, and 40° of data were collected with an oscillation of 1°. The crystal parameters and data collection statistics of con-T[K7γ] are listed in Table 1.

(9) Li, X. Q.; Suzukim, K.; Kanaori, K.; Tajima, K.; Kashiwada, A.; Hiroaki, H.; Kohda, D.; Tanaka, T. *Protein Sci.* **2000**, *9*, 1327−1333.
(10) Kiyokawa, T.; Kanaori, K.; Tajima, K.; Koike, M.; Mizuno, T.; Oku, J.; Tanaka, T. *J. Pept. Res.* **2004**, *63*, 347−353.
(11) Handel, T.; Williams, S. A.; Degrado, W. F. *Science* **1993**, *261*, 879−885.
(12) Kohn, W. D.; Kay, C. M.; Sykes, B. D.; Hodges, R. S. *J. Am. Chem. Soc.* **1998**, *120*, 1124−1132.
(13) Dai, Q.; Prorok, M.; Castellino, F. J. *J. Mol. Biol.* **2004**, *336*, 731−744.
(14) McIntosh, J.; Olivera, B. M.; Cruz, L.; Gray, W. *J. Biol. Chem.* **1984**, *259*, 14343−14346.
(15) Castellino, F. J.; Prorok, M. *Curr. Drug Targets* **2000**, *1*, 219−235.
(16) Warder, S. E.; Blandl, T.; Klein, R. C.; Castellino, F. J.; Prorok, M. *J. Neurochem.* **2001**, *77*, 812−822.
(17) Dai, Q.; Castellino, F. J.; Prorok, M. *Biochemistry* **2004**, *43*, 13225−13232.
(18) Otwinowski, Z. In *Proceedings of the CCP4 Study Weekend*; Sawyer, L., Issacs, N., Bailey, S., Eds.; SERC Daresbury Laboratory: Warrington, UK, 1993; pp 56−62.
(19) Otwinowski, Z. *Methods Enzymol.* **1997**, *276*, 307−326.

Table 1. Data Collection and Refinement Statistics for the Ca^{2+}/con-G and Ca^{2+}/con-T[K7γ] Complexes

	Ca^{2+}/con-G	Ca^{2+}/con-T[K7γ]
	Data Collection	
space group	$P4_222$	$P4_332$
cell dimensions		
a, *b*, *c* (Å)	29.3, 29.3, 46.9	89.0, 89.0, 89.0
α, β, γ (deg)	90.0, 90.0, 90.0	90.0, 90.0, 90.0
resolution (Å)[a]	1.2(1.29−1.24)	1.6(1.66−1.60)
R_{merge}	7.9	9.8
$I/\sigma I$[a]	20.91(1.31)	21.31(1.88)
completeness (%)[a]	97.9(97.7)	99.5(99.5)
	Refinement	
resolution (Å)	8−1.25	10−1.7
no. measured reflections	266169	215476
no. unique reflections	12427	16539
R_{work}/R_{free}	11.99/16.15	13.35/18.63
no. atoms		
protein	168	378
Ca^{2+}	3	4
water	68	142
mean B-factors (Å^2)	28.58	34.56
rms deviations		
bond lengths (Å)	0.010	0.011
angle distances (Å)	0.024	0.033

[a] Highest resolution shell is shown in parentheses.

Structure Determination. Both structures were solved by molecular replacement using the program Phaser[20] and a 14-mer polyalanine helix as a model. The Matthews coefficient for con-G was 2.3 with 46% solvent content predicting a single molecule in the asymmetric unit. For con-G, brute force rotation and translation functions were performed, followed by refinement. The translation *Z*-score and log likelihood gain (LLG) were 6.83 and 48.46, respectively. The LLG score after refinement improved to 63.82. For con-T[K7γ], the Matthews coefficient was 4.3 and 71.3% solvent for two molecules in the asymmetric unit. Automated searches using Phaser[20] were performed to find the correct solutions. The translation *Z*-score and LLG for the first molecule were 8.6 and 57, respectively, and 19.1 and 216 for the second molecule. Phaser[20] proved to be the only molecular replacement program capable of locating a correct solution, as many other programs failed.

Refinement of con-G. A rigid body refinement was performed using Refmac5[21] within the CCP4 suite of programs,[22] producing an R_{work} value of 53.7% and R_{free} value of 54.6%. Side chains were built into the structure from the electron density map. Subsequent refinements of all 17 residues of con-G led to an R_{work} value of 35.9% and R_{free} value of 45.4%. To determine the positions of the Ca^{2+} ions, an $F_o - F_c$ map was calculated and contoured at 8σ. This map showed that three Ca^{2+} ions were present within the structure. After these ions were added, refinement was performed where the R_{work} and R_{free} values dropped to 27.16 and 32.29%, respectively. Arp/warp[21,23] was then used to add water molecules. Further cycles of refinement using the Refmac5[21] program in CCP4[22] produced an R_{work} value of 18.22% and R_{free} value of 21.37%. The program SHELXL-97[24] was then employed. Additional water molecules were included, and secondary side-chain conformations for residues L5, Q9, and S16 were added to the refinement. SHELXL produced final R_{work} and R_{free} values of 11.99 and 16.15%, respectively.

(20) McCoy, A. J.; Grosse-Kunstleve, R. W.; Storoni, L. C.; Read, R. J. *Acta Crystallogr.* **2005**, *D61*, 458−464.
(21) Murshudov, G. N.; Vagin, A. A.; Dodson, E. J. *Acta Crystallogr.* **1997**, *D53*, 240−255.
(22) Collaborative Computational Project, N. *Acta Crystallogr.* **1994**, *D50*, 760−763.
(23) Perrakis, A.; Morris, R. J. H.; Lamzin, V. S. *Nat. Struct. Biol.* **1999**, *6*, 458−463.
(24) Sheldrick, G. M.; Schneider, T. R. In *Macromolecular Crystallography*; Sweet, R. M., Carter, C. W., Jr., Eds.; Methods in Enzymology 277; Academic Press: San Diego, CA, 1997; pp 319−343.

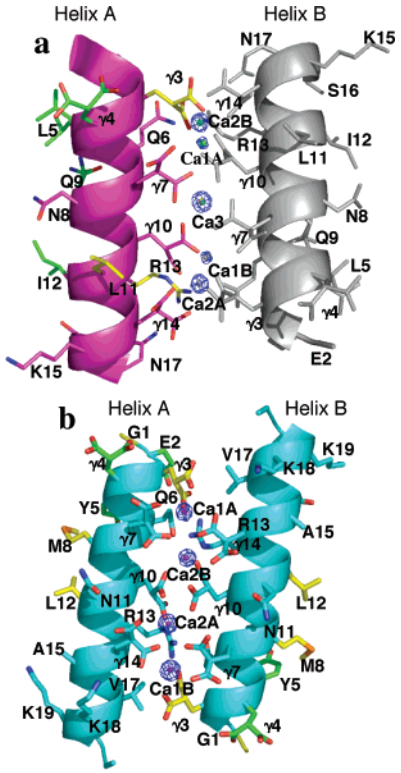

Figure 1. Three-dimensional structures of con-G and con-T[K7γ]. (a) Overall structure of the con-G dimer with a $F_o - F_c$ map calculated in the absence of Ca^{2+} and contoured at 8σ. The gray molecule is related by crystallographic twofold symmetry that forms the dimer. Green side chains (E2, γ4, L5, Q9, I12) have been shown to decrease NMDA receptor inhibitory potency by at least 100-fold when replaced with Ala. Yellow side chains (G1, γ3, L11, R13) decrease NMDA receptor inhibitory potency by at least 10−60-fold when replaced with Ala. Magenta side chains have minimal impact on NMDA receptor inhibition upon replacement with Ala. Ca3 is positioned directly on the crystallographic twofold axis. Ca1A and Ca2A are crystallographically related to Ca1B and Ca2B, respectively. (b) The overall structure of con-T[K7γ] with a $F_o - F_c$ map calculated in the absence of Ca^{2+} and contoured at 8σ. Green side chains (E2, γ4, Y5) decrease NMDA receptor inhibitory potency by at least 100-fold when replaced with Ala. Yellow side chains (G1, γ3, M8, L12) decrease NMDA receptor inhibitory potency by at least 10−60-fold when replaced with Ala. Cyan side chains have minimal impact on NMDA receptor inhibition upon replacement with Ala. In all cases, the peptide side-chain heteroatoms are colored by atom type.

Refinement of con-T[K7γ]. A rigid body refinement was performed as above, producing an R_{work} value of 52.5% and R_{free} value of 56.5%. After building in side chains and adding Ca^{2+} and water molecules, we obtained an R_{work} value of 20.36% and R_{free} value of 23.08%. To finalize refinement of the structure, SHELXL-97[24] was employed, producing final R_{work} and R_{free} values of 13.35 and 18.63%, respectively. Both structures have been deposited in the Protein Data Bank (access codes 2DPQ and 2DPR, respectively).

Results

The X-ray crystal structures of the Ca^{2+}/con-G and Ca^{2+}/con-T[K7γ] have been determined at high resolution. Their overall structures are shown in Figure 1a,b, respectively. The con-G α-helix is approximately 26 Å in length. A total of three Ca^{2+}, one Cl^-, and 68 water molecules were included in the model. Secondary side-chain conformations exist for con-G residues, Leu5, Gln9, and Ser16. The con-T[K7γ] α-helix is approximately 30 Å in length with a total of four Ca^{2+} and 142 water molecules.

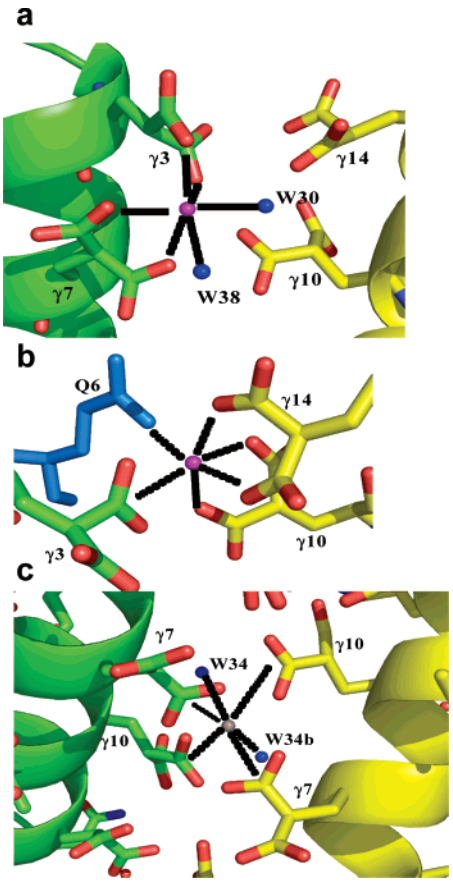

Figure 2. Ca^{2+} coordination in con-G. (a) Ca1A (magenta) coordinates with γ3 and γ7 as well as two water molecules, W30 and W38 (blue). Ca1A does not coordinate with any residues from the crystallographically related helix. The crystallographically related helix forming the dimer is yellow. (b) Ca2B (magenta) coordinates with γ3 and Q6 of helix A and γ14 and γ10 of the crystallographically related helix B forming the dimer. Ca2A does not coordinate with any water molecules. The symmetry-related crystallographic helix forming the dimer is yellow. Q6 is displayed in blue. (c) Ca3 (gray) lies directly on the crystallographic twofold axis and coordinates with γ7 and y10 of each helix as well as with waters W34 and W34b (blue), a symmetry-related water molecule. The symmetry-related helix forming the dimer is yellow. In all cases, the peptide side-chain atoms are colored by atom type, except as otherwise indicated.

Structure of Ca^{2+}/con-G. In the presence of Ca^{2+}, con-G forms an antiparallel dimeric structure (Figure 1a). Four of the Gla residues (3, 7, 10, 14) are present on one face of the helix, specifically the Ca^{2+} coordination interface, while Gla4 resides on the opposite side of the helix and does not coordinate Ca^{2+}. A crystallographic twofold axis passes through Ca3, the central Ca^{2+} ion, relating the two helices to form a dimer. Therefore, the con-G dimer contains five Ca^{2+}, two associated with each of the crystallographically equivalent helices, and one shared between the two that are bisected by a crystallographic twofold axis. The two helices are referred to as helix A and helix B, for the unique and crystallographically equivalent helix, respectively. Ca^{2+} ions are designated as Ca1A, Ca2A, Ca1B, Ca2B, and Ca3, for those associated with helix A, helix B, and shared, respectively. Ca1A and Ca1B and Ca2A and Ca2B are related by crystallographic symmetry, as are helix A and helix B. Ca1A (and by symmetry Ca1B) is coordinated by both carboxylates of two Gla residues, Gla3 and Gla7, accounting for a total of four ligands to Ca1A (Figure 2a). Similarly, Ca2A (or Ca2B on helix B) is chelated by Gla10 and Gla14, with all four carboxylates of the two Gla residues acting as ligands (Figure 2b). Both Ca1A and Ca2A have octahedral geometry with the two carboxylates of a single Gla residue occupying coordination sites separated by about 90°. The central Ca^{2+} ion, Ca3, is also coordinated by two Gla residues, Gla7 and Gla10, but each Gla residue donates only one carboxylate to Ca3 (Figure 2c). Therefore, helix A donates a total of only two ligands to Ca3. There is an identical arrangement of chelated Ca^{2+} ions on helix B, as required by the crystallographic symmetry relating the two helices. It is clear that the helical conformation is stabilized by the metal-mediated interactions of Gla residues located one helical turn apart. Metal chelation enforces the positioning of all four Gla residues and, by nature of the Ca3 chelation of Gla7 and Gla10, enforces the location of all four Gla residues on a single helical face. A similar chelation arrangement is likely for other metal ions, such as Mg^{2+}, which also leads to a helical conformation in con-G. Absent metal ions, the electrostatic repulsion caused by the concentration of negative charges from the Gla residues on a single helical face would destabilize a helical conformation, consistent with all biophysical measurements that show that con-G is not helical in the absence of metal ions.[25−29]

The dimerization interface between helix A and helix B is defined almost exclusively by intermolecular Ca^{2+} coordination between the two helices. There are no direct contacts between residues of the two helices, although there are some water-mediated interactions (vide infra). Three of the five Ca^{2+}, Ca2A, Ca2B, and Ca3, are involved in intermolecular coordination. Helix B donates two ligands to Ca2A, the side-chain carbonyl oxygen of Gln6 and a single carboxylate group of Gla3 (Figure 2b). This creates an octahedral coordination geometry about Gla3, with two of the six ligands originating from helix B. Since Ca3 resides on a crystallographic twofold axis that relates helix A with helix B, the coordination of Ca3 to helix B is identical to that of Ca3 to helix A. This results in four carboxylate ligands, one each from Gla7 and Gla10 from each of the two helices acting as ligands for Ca3. The other two coordination sites of Ca3 are occupied by water molecules to complete the octahedral geometry. The other two Ca^{2+}, Ca1A and Ca1B, do not participate in interhelical contacts (Figure 2a), though mutational studies indicate that their ligands, Gla3 and Gla7, are both important for Ca^{2+}-mediated helix dimerization.[13] This is most likely due to the induction of a stable monomeric helix upon occupation of the Ca1A/Ca1B site formed by Gla3 and Gla7.

Structure of Ca^{2+}/con-T[K7γ]. Unlike con-G, there is no crystallographic twofold symmetry relating the helices of the con-T[K7γ] dimer, although the two con-T[K7γ] helices are virtually identical (overlay in Figure 3a). The Ca^{2+} coordination within each con-T[K7γ] helix is also identical. There are four Ca^{2+} bound to the con-T[K7γ] helix, Ca1A and Ca2A, which are predominantly associated with helix A, and Ca1B and Ca2B, which are associated with helix B of the dimer. As occurs with Ca1A and helix A of con-G, Ca1A coordinates helix A of con-

(25) Prorok, M.; Warder, S. E.; Blandl, T.; Castellino, F. J. *Biochemistry* **1996**, *35*, 16528−16534.
(26) Skjaerbaek, N.; Nielsen, K. J.; Lewis, R. J.; Alewood, P.; Craik, D. J. *J. Biol. Chem.* **1997**, *272*, 2291−2299.
(27) Rigby, A. C.; Baleja, J. D.; Furie, B. C.; Furie, B. *Biochemistry* **1997**, *36*, 6906−6914.
(28) Rigby, A. C.; Baleja, J. D.; Li, L.; Pedersen, L. G.; Furie, B. C.; Furie, B. *Biochemistry* **1997**, *36*, 15677−15684.
(29) Warder, S. E.; Prorok, M.; Chen, Z.; Li, L.; Zhu, Y.; Pedersen, L. G.; Ni, F.; Castellino, F. J. *J. Biol. Chem.* **1998**, *273*, 7512−7522.

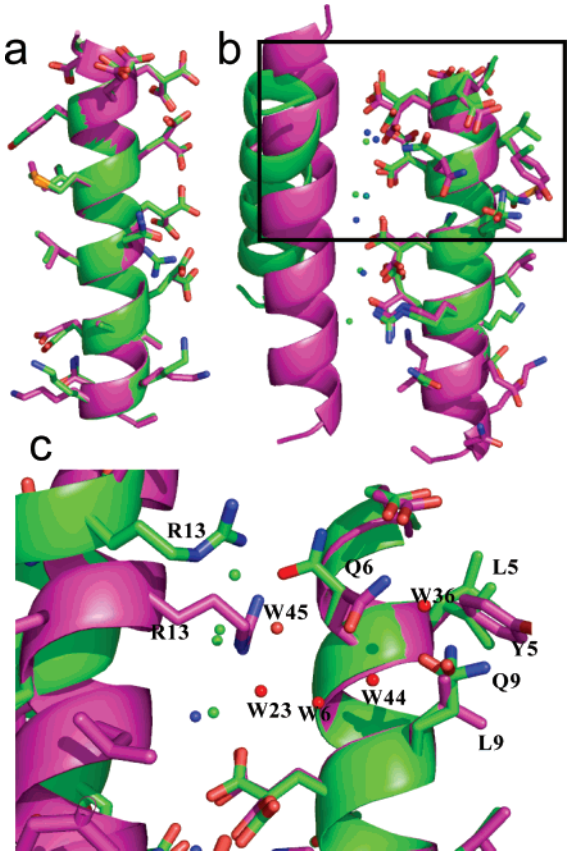

Figure 3. Comparison of the con-T[K7γ] and con-G helices. (a) Overlay of the two con-T(K7γ) helices shows their identity. (b) Overlay of the con-T[K7γ] (magenta) and con-G (green) helices demonstrates that these helices are nearly identical to each other. Blue spheres represent Ca^{2+} ions of con-G, and green spheres designate Ca^{2+} ions of con-T[K7γ]. Note that two of the con-G calcium ions overlap in this view, obscuring one of them. (c) The boxed area in (b) is magnified and includes waters (red spheres). In all cases, the peptide side-chain heteroatoms are colored by atom type.

T[K7γ] via a tetravalent interaction between all of the carboxylate residues of Gla3 and Gla7. The analogous scheme exists for Ca2A, which chelates all four carboxylates of Gla10 and Gla14 of helix A, resulting in an interaction essentially identical to that seen for Ca2A of con-G. Ca1B and Ca2B of con-T[K7γ] are correspondingly identical to Ca1B and Ca2B of con-G.

Taken together, it is clear that when a single helix is viewed in isolation, the con-G and con-T[K7γ] structures are very similar, except that Ca3 appears to be missing in the con-T[K7γ] structure (Figure 3b,c).

The dimerization interface of con-T[K7γ] is not similar to that of con-G. Given the structural similarity between con-G and con-T[K7γ], it was surprising to observe a difference in the dimer interface between the two structures. While both peptides yield antiparallel helical dimers and both are largely stabilized by Ca^{2+}-mediated chelation, the relative orientation of the helices as well as the Ca^{2+} coordination in the interface are radically different in the con-T variant (overlays in Figure 3b,c).

The two helices of con-T[K7γ] are almost parallel, and all four Ca^{2+} are involved in the dimerization interface of con-T[K7γ]. As seen in Figure 4a, Ca1A, chelated by Gla3 and Gla7 of helix A, coordinates one carboxylate of Gla14 of helix B, while Ca2A, chelated by Gla10 and Gla14 of helix A, coordinates one carboxylate each of Gla7 and Gla10 of helix B

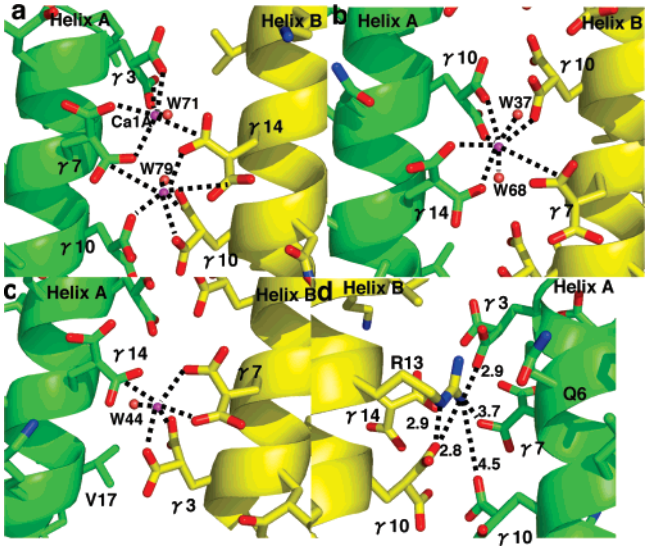

Figure 4. Ca^{2+} coordination in the con-T[K7γ] dimer. (a) Ca1A (magenta) coordinates with γ3 and γ7 of helix A and γ14 of helix B, as well as with one water molecule, W71 (red sphere). Ca2B (magenta) coordinates with γ7 and γ10 of helix A and γ14 and γ10 of helix B, along with water molecule W79 (red sphere). (b) Ca2A (magenta) coordinates with γ10 and γ14 of helix A and γ10 and γ7 of helix B. Ca2A also coordinates with two water molecules, W37 and W68 (red spheres). (c) Ca1B (magenta) coordinates with γ14 of helix A and γ7 and γ3 of helix B. Ca1B (magenta) also coordinates with one water molecule, W44 (red sphere). (d) The salt bridge interactions in con-T[K7γ]. All distances are shown in angstroms. In each case, the peptide side-chain heteroatoms are colored by atom type.

(Figure 4b). The coordination sphere of Ca1B is identical to that of Ca1A (Figure 4c), and the coordination sphere of Ca2B (Figure 4a) is identical to that of Ca2A, except that the residues of helix A are transposed for the residues of helix B. The result of this chelation pattern is that the two helices are staggered by approximately one helical turn along the collinear helix axes and the Gla residues account for all of the Ca^{2+} chelation in con-T[K7γ]. In addition to the Ca^{2+} interactions, a short salt bridge exists between Arg13 of helix A and Gla3 of helix B and an identical salt bridge is formed between Arg13 of helix B and Gla3 of helix A to complete the symmetric interaction (Figure 4d).

A further stabilization of the con-T[K7γ] dimeric structure involves a spine of water molecules that runs between the Ca^{2+}, from Ca1A to Ca1B (Figure 5a), all of which are chelated by Ca^{2+}. This continuous spine of hydration is not seen in the con-G structure. The fundamental differences between the dimer interface in con-G versus con-T[K7γ] are illustrated by the schematic "wiring diagram" presented in Figure 5b. First, there is a clear correspondence between Ca1A, Ca1B, Ca2A, and Ca2B in all of the structures, since they have identical chelation from one of the two helices. For example, all Ca1-type ions are chelated to Gla3 and Gla7 of a single helix by both of their carboxylate moieties, while Ca2-type ions are chelated to Gla10 and Gla14 of a single helix by both of their carboxylate moieties. In addition, all four helices coordinate a single Ca^{2+} via Gla7 and Gla10 in bidentate fashion, using only one carboxylate from each Gla. Therefore, if any of the four helices are viewed in isolation, the Ca^{2+} coordination appears to be identical. The dramatic difference occurs because each Ca^{2+} interacts differently with the adjacent helix in the two structures. For example, in con-T[K7γ] all Ca1-type ions chelate with a single carboxylate of Gla14 on the partner helix, thus creating a symmetric

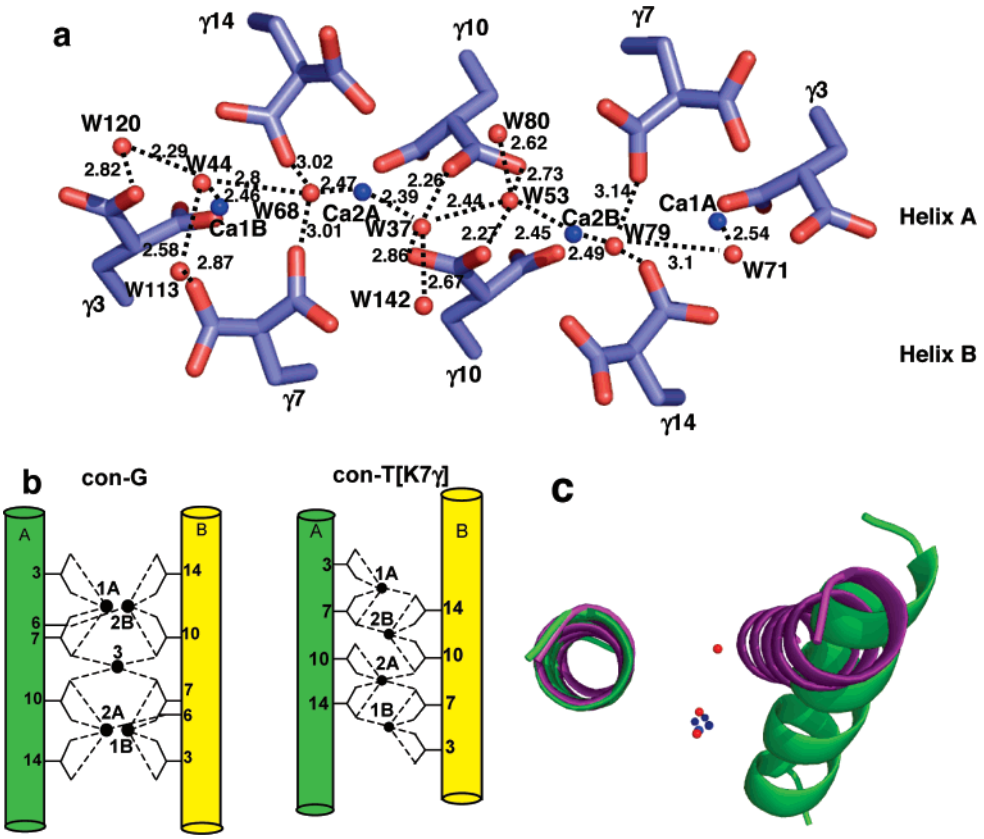

Figure 5. con-T[K7γ] dimer interface is significantly different from that of con-G. (a) A water network exists at the Ca^{2+}/dimer interface of Ca^{2+}/con-T[K7γ]. All distances are shown in angstroms. The Ca^{2+} ions are shown as blue spheres, and the waters are shown as red spheres. The top four Gla residues belong to helix A, and the bottom four Gla residues belong to helix B. (b) The fundamental differences between the Ca^{2+}/con-G structure and Ca^{2+}/con-T[K7γ] structure are shown in a schematic wiring diagram. Each dotted line represents a coordination between one Gla carboxylate and a Ca^{2+}. (c) Overlay of the con-G and con-T[K7γ] structures showing difference in helix alignment. The con-G dimer is green, and its Ca^{2+} ions are red. The con-T[K7γ] dimer is magenta, and its Ca^{2+} ions are blue. In all cases, peptide side-chain heteroatoms are colored by atom.

interaction. On the other hand, in con-G Ca1-type ions do not chelate with their partner helix. Furthermore, the Ca2-type ions of con-T[K7γ] chelate Gla7 and Gla10 of their partner helix, while in con-G, the Ca2-type ions chelate the side chain of Gln6, while Ca3 coordinates Gla7 and Gla10 residues from both helices. The result of this coordination difference is to cause the con-G helices to be twisted out of plane to accommodate the octahedral coordination about Ca3, while the helices in con-T[K7γ] are parallel, but are shifted along the helix axis by one turn to accommodate the chelation of both Ca1 and Ca2 (Figure 5c).

Discussion

While both con-G and the variant con-T (con-T[K7γ]) provide an identical Gla pattern that allows antiparallel dimerization in the presence of Ca^{2+} and would therefore be expected to yield similar Ca^{2+}-bridged dimeric interfaces, this was not the case. There is a substantial difference in dimerization and Ca^{2+} affinity between these two peptides. In fact, con-T[K7γ] exhibits a 10-fold higher association constant for dimerization and 10-fold higher affinity for Ca^{2+} than con-G.[17] This is consistent with the present structures as there are four Ca^{2+} in the dimer interface of con-T[K7γ] and only three in con-G. There are also more bridging interactions in con-T[K7γ], with six cross-helix ligand interactions compared to only four in con-G (these are Ca^{2+}-mediated interactions where the metal ion is assumed to be bound to one of the helices and coordination sites to the partner helix are counted). There are also two tight salt-bridge interactions (involving Arg13 and Gla3) between helices in con-T[K7γ] that are not seen in con-G. There is also a spine of water molecules that span all four Ca^{2+} in con-T. Each of the six water molecules that constitute this spine is coordinated by one of the four Ca^{2+} ions. This spine of hydration is absent in the con-G structure, at least partly because the Ca^{2+} ions in con-G have fewer coordinated water molecules. Taken together, these observations are consistent with the higher binding and dimerization affinity of con-T[K7γ] compared to that of con-G. Another potential contributing factor to the difference in dimer interface is the burial of Val17 within the interface in the con-T[K7γ] dimer versus the solvent-exposed position of the analogous Gln17 residue in con-G. However, Val17 is only partially buried in con-T[K7γ] and is actually close to three well-ordered surface water molecules. Furthermore, it is closest not to another hydrophobic residue in the interface but to the charged γ3, which is not expected to yield a particularly favorable interaction. For these reasons, it is not expected that Val17 plays the most dominant role in dimer interface selection.

Our structure is also consistent with the fact that native con-T binds Ca^{2+} without dimerization.[13] The absence of Gla7 destabilizes, if not eliminates, the Ca2 and Ca4 binding sites, leading to loss of two helix-bridging interactions to Gla14. Gla7 is also involved in helix-bridging interactions to Ca2 and Ca3. Therefore, removal of this residue leads to probable loss of three of the helix-bridging interactions observed in the structure. It

is interesting to note that metal-free native con-T has significant helical content as opposed to both con-G and con-T[K7γ]. This is probably due to two factors. First, electrostatic repulsions between the four Gla residues on one side of a helix almost certainly lead to destabilization. Gla7 contributes significantly to this destabilization because it resides in the center of the helix. Replacement of Gla7 with a positively charged side chain (e.g., Lys) would significantly reduce this electrostatic repulsion and may possibly add electrostatic stabilization by forming salt-bridging interactions with both Gla3 and Gla10. Consistent with this is the fact that the con-G[γ7K] mutant is significantly more helical in the absence of metal ions than is native con-G.[30] The con-T peptide is also four residues longer than con-G, and all of these residues are helical in the crystal structure. It is well-accepted that longer helices are more stable than shorter helices.

Less clear is what causes the different dimerization interface of con-T[K7γ] relative to con-G. Although eight amino acids differ between the two peptides, all of the residues that are involved in Ca^{2+} binding and dimerization are conserved. The overlay of the con-G and con-T[K7γ] helices shows that most of the residues in the interface have identical conformations in the two structures. The most significant difference is in the conformation of Gln6, which is flipped into the interface and chelates Ca2B (or Ca2A for the B helix) in con-G, but is flipped out of the interface in con-T[K7γ] and interacts with Tyr5, a residue that is not conserved in the two peptides. Hence, the conformation of Gln6 appears to be critical to both dimer interfaces. As one of the cross-helical Ca^{2+} ligands in the con-G interface, the flipped-out Gln6 conformation would compromise this mode of Ca^{2+} coordination. On the other hand, in con-T[K7γ], the flipped-in conformation of Gln6 would sterically clash with Arg13 from the other helix and prevent the formation of the salt bridge between Arg13 and Gla3 in con-T[K7γ]. Overlaying the two helices indicates that the Gln6 flipped-out conformation is opposed in con-G by both the conformation of Gln9, which is also not conserved in con-T, and the resulting water structure around Gln9 and Glu2. The flipped-out conformation would bring the Gln6 side-chain oxygen atom within 3 Å of the Gln9 oxygen atom and within 2 Å of two very well-ordered water molecules that form a bridge between Glu2 and Gln9, all of which represent electrostratic and steric clashes. The side-chain oxygens of both Gln6 and Gln9 are well-defined, since the Gln6 side-chain nitrogen must interact with Glu2, and the Gln9 nitrogen must interact with the main-chain carbonyl of Leu5. Therefore, the dimer interface is defined primarily by the metal chelation of the four critical Gla residues, Gla3, 7, 10, and 14, but is also strongly affected by subtle, indirect effects on the conformation of other side chains as well.

Mutational Studies of the con-G and con-T Peptides. The systematic mutational studies of both con-G and con-T[16,30] have shed much light on our structural results. For example, deletion of residues from the C-terminus of either the con-T or con-G helices leads to reduced helicity. This is not surprising given that longer helices are usually found to be more stable than shorter ones and our structure demonstrates that an end-to-end helix exists for both peptides. Furthermore, individual replacement of Gla residues 3, 7, 10, or 14 leads to significantly reduced helicity for con-G,[30] consistent with our observation that chelation of Ca^{2+} to these residues defines and stabilizes the helical peptide structure. Though replacement of many of the other residues also leads to some loss of helicity, it is particularly interesting to note that, in con-G, the R13A variant manifests a nearly complete loss of helicity in the presence of Ca^{2+}. In the case of con-T, the R13A replacement likewise diminishes the helix content of both Ca^{2+}-bound and metal-free peptide forms.[16,30] In our structure, Arg13 makes a tight salt bridge with Gla10 of the same helix in both con-G and con-T[K7γ] and in the latter makes an additional salt bridge with Gla3 of the adjoining helix. It thus appears that Arg13 is important for stabilization of the dimer form, through neutralization of the considerable negative charge within the helix−helix interface, and also participates in intrapeptide electrostatic contacts that stabilize the monomeric form of apo con-T.

The con-G and con-T Structures and NMDA Receptor Binding. Those residues found by alanine replacement to be important for NMDA receptor binding or antagonism define one face of both the con-G and con-T helices (Figure 1a,b).[16] The N-termini of the peptides are especially critical for biological activity, consistent with the fact that the N-termini of con-T and con-G are identical through the first four residues. Gla4 is particularly important, since mutation of this residue, even conservatively to Asp or Glu, results in no detectable NMDA receptor activity.[16] The fact that these residues are localized to one face of the helix strongly indicates that both peptides bind the receptor in a helical conformation, even though replacements that significantly destabilize the con-G or con-T helix do not always have a significant effect on NMDA receptor binding (e.g., γ10A). However, for both con-G and con-T, the γ3A replacement results in the reduction of IC_{50} values by at least an order of magnitude. Our hypothesis is that NMDA receptor binding is most dependent on the maintenance of the helical conformation in the N-terminus of the helix. Alanine replacement of γ3 results in helix fraying at the N-terminus, possibly through loss of the stabilizing effect that the negatively charged Gla residue imparts to the helix macrodipole at the N-terminus, thereby reducing peptide affinity for the receptor. In further support of the helical hypothesis is con-G[γ7P], which is incapable of helix formation and is completely inactive at the NMDA receptor.[30] On the other hand, the C-terminal part of the helix is less critical for interaction, and therefore loss of helicity in this region is less deleterious to receptor binding.

Comparison of the Crystal Structures to the NMR Structures. Several NMR-based structures of both metal-bound and apo forms of con-T and con-G have been determined.[26−29,31,32] Most relevant to this discussion are the NMR-derived structures of Ca^{2+}-complexed con-G.[25−27] While the helical backbones of these structures are very similar to the X-ray structure determined herein (Figure 6), neither of the NMR-derived structures predicts the dimerization interface. This is consistent with our data, which indicate that there are no interhelical proton distances closer than 5 Å. This would obviate detection of the dimeric species by 2D NMR, since NOEs do not typically evolve from proton−proton distances with the mixing time employed in the afore-referenced studies. While side-chain orientations on the Gla-rich face of the helix are similar between the NMR and X-ray structures, profound differences are

(30) Blandl, T.; Prorok, M.; Castellino, F. J. *FEBS Lett.* **1998**, *435*, 257−262.
(31) Warder, S. E.; Chen, Z.; Zhu, Y.; Prorok, M.; Castellino, F. J.; Ni, F. *FEBS Lett.* **1997**, *411*, 19−26.
(32) Chen, Z.; Blandl, T.; Prorok, M.; Warder, S. E.; Li, L.; Zhu, Y.; Pedersen, L. G.; Ni, F.; Castellino, F. J. *J. Biol. Chem.* **1998**, *273*, 16248−16258.

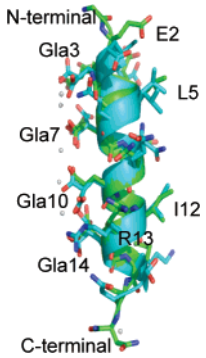

Figure 6. Overlay of the NMR and X-ray crystal structures of Ca^{2+}/con-G. Cyan, the X-ray structure from this report; green, a low-energy NMR structure;[27] white, Ca^{2+}. In all cases, peptide side-chain heteroatoms are colored by atom type.

observed at the opposite face and at the termini. These latter disparities likely reflect some of the uncertainties involved in garnering NMR-based structural information in the more flexible regions of the peptide, wherein an ensemble of solution conformers must be averaged. Furthermore, computational docking of Ca^{2+} into the structure of con-G[27] yields stoichiometry and placement that is different from that associated with the crystal structure. A total of four bound Ca^{2+} are predicted from the NMR data, whereas three exist per monomer in the crystal structure. While three of these Ca^{2+} ions form a similar coordination network in both structures, the NMR-derived complex deviates from our structure in that it invokes Gla3 and Gla4 as ligands for a fourth Ca^{2+}. Also, the Ca^{2+}-docked NMR structure does not reveal Ca^{2+} coordination to the side-chain carbonyl of Gln6 of con-G.

It is difficult to accurately predict metal positions in peptides and proteins solely by using conventional NMR in tandem with modeling techniques. While single-crystal X-ray diffraction is a powerful approach for elucidating the subtle details of metal ion binding, it is not without uncertainties caused by the structural ramifications of crystal packing interactions, whereas dynamic solution structures are without these constraints. Thus, both approaches continue to provide value and some differences using such disparate approaches should be expected.

In conclusion, limited success has been obtained in the past in the design of short peptides that adopt stable, structurally homogeneous α-helical conformations. Almost all helices are stabilized by the hydrophobic effect, promoting the formation of a hydrophobic helical face that is critical to stabilize the structure. It is also the primary force that drives helix self-assembly as seen in coiled coil multimers (e.g., the leucine zipper motif). A possible alternative to the hydrophobic effect is the use of metal ion coordination to electrostatically stabilize the helical conformation. However, to date, there are no examples of a peptide that is solely dependent on metal ion chelation for both helix formation and self-assembly. Further, there were no high-resolution crystal structures of any of the metal-promoted helices, leaving open the full nature of the metal coordination. Employing the con-G and con-T[K7γ] peptides, we provide the first example of helix stabilization and self-assembly that is completely dependent on electrostatics and metal coordination, with no component of the stabilization due to the hydrophobic effect. The unique dispensation of Gla residues on one face of the helix, resulting in a regular coordination of metal ions along this face, gives rise to this effect, resulting in what we call a "metallo-zipper motif". In addition, the natural peptides form specific antiparallel helix dimers in the presence of Ca^{2+} and fold into monomeric helices in the presence of Mg^{2+}. Our structures of these peptides show very clearly the nature of the metal chelation that leads to helix formation and also elaborate the dimerization interface in both peptides. The structures also demonstrate that while the metal chelation is very similar in the two peptides, they surprisingly result in completely different dimer interfaces. The dimer interface appears to be exquisitely sensitive to amino acid changes that are not directly involved in the metal chelation that results in dimerization. This is the first example of a short peptide helix that is completely stabilized by metal ion chelation. Helix formation depends only on the disposition of the metal-chelating Gla residues. The dimer interface consists exclusively of metal coordination interactions in the case of the con-G dimer, while a salt bridge interaction plays an important role in defining the con-T[K7γ] interface. These structures provide a fertile platform for the design of short peptide helices that are comparatively insensitive to amino acid sequence in all but a few positions. The structures also provide a much better understanding of the mechanism of metal-dependent oligomerization.

Acknowledgment. This work was supported by Grant GR-179 (085P100549) from the Michigan Economic Development Corporation (J.H.G.), NIH Grant HL019982 (F.J.C.), and NIH Grant GM0638947 (J.H.G.).

JA065722Q